

# The inertial damping of the VIRGO superattenuator and the residual motion of the mirror

The VIRGO Collaboration (presented by Giovanni Losurdo<sup>1</sup>)

<sup>1</sup> Istituto Nazionale di Fisica Nucleare—Sezione di Firenze, Lgo E Fermi, 2, Firenze, Italy

E-mail: losurdo@virgo.infn.it

Received 9 November 2001, in final form 6 December 2001

Published 14 March 2002

Online at [stacks.iop.org/CQG/19/1631](http://stacks.iop.org/CQG/19/1631)

## Abstract

The VIRGO superattenuator (SA) is effective in suppressing seismic noise below the expected thermal noise level above 4 Hz. However, the residual mirror motion associated with the SA normal modes can saturate the interferometer control system. This motion is reduced by implementing a wideband (DC–5 Hz) multidimensional active control (the so-called *inertial damping*) which makes use of both accelerometers and position sensors and of a digital signal processing (DSP) system. Feedback forces are exerted by coil–magnet actuators on the top of an inverted pendulum pre-isolator stage. The residual root mean square motion of the mirror in 10 s is less than 0.1  $\mu\text{m}$ .

PACS number: 0480N

(Some figures in this article are in colour only in the electronic version)

## 1. Introduction

The test mass suspension of the VIRGO detector, the superattenuator (SA) [1], has been designed in order to suppress seismic noise below the thermal noise level above 4 Hz. The expected residual motion of the mirror is  $\sim 10^{-18} \text{ m Hz}^{-1/2}$  at 10 Hz. At lower frequencies, in the range of the normal modes of the SA (0.04–2 Hz), the residual motion of the mirror is much larger (tens of microns).

In order to avoid saturation of the readout electronics of the VIRGO interferometer, the tolerable root mean square (rms) motion of the suspended mirrors is  $\sim 10^{-12} \text{ m}$ . A hierarchical control strategy is needed to cover the entire dynamic range (for a nice introduction to this problem see [2]): feedback forces can be exerted on three points of the SA (the inverted pendulum (IP) [3], the *marionette* [4, 5] and the mirror itself, by means of a recoil mass). The control on the three points is operated in different ranges of frequency and amplitude. The IP will be used to compensate for low frequency motions (below 0.1 Hz). The marionette will be used up to a few hertz. The requirement that the control does not inject noise in the VIRGO

detection band and the limited dynamic range of the control, sets a limit to the maximum displacement that can be compensated by the marionette. The residual motion of the mirror in the Hz region is associated with the resonances of the SA. Active control of the SA normal modes, using sensors and actuators on top of the IP, capable of reducing the mirror residual motion to the level of  $0.1 \mu\text{m}$  in 10 s, has been successfully implemented.

## 2. Inertial damping

Each superattenuator (figure 1) is provided with three accelerometers [6] (placed on top of the IP), three linear variable differential transformer position sensors (LVDT) [7], measuring the relative motion of the IP with respect to an external frame and three coil–magnet actuators. The sensors and actuators are all placed in a *pin-wheel* configuration. The sensor and actuator signals are processed by a computer controlled ADC (16 bit)–DSP–DAC (20 bit) system.

The active control of the SA normal modes is defined as *inertial damping*, because it makes use of inertial sensors (accelerometers) to sense the SA motion. Inertial sensors are used so that no seismic noise is re-injected by the feedback. Actually, in the real SA control, both sensors are used: position sensors provide a low frequency (DC–30 mHz) control of the SA position (in order to avoid drifts), while accelerometers allow a wideband reduction of the noise in the region of the SA resonances (30 mHz to 5 Hz).

The object to control is a MIMO (multiple in multiple out) system: each sensor (accelerometer/LVDT) is sensitive to the three modes ( $X$ ,  $Y$ ,  $\Theta$ ) of the IP and each actuator excites all the modes. To simplify the control strategy, the sensor outputs and the actuator currents are digitally recombined to obtain independent SISO (single in single out) systems: the system is described in normal mode coordinates (a detailed description of the experimental set-up, the diagonalization procedure, the control strategy and the inertial damping performance is given in [8]). Each normal mode is associated with a so-called *virtual sensor* (sensitive to that mode and ‘blind’ to the others) and a *virtual actuator* (acting on one mode only, leaving the others undisturbed). In this way one is able to implement independent feedback loops on each degree of freedom (d.o.f.), greatly simplifying the control strategy.

## 3. Inertial damping performance

The result of inertial control on one of the VIRGO superattenuators is shown in figure 2. The measurement was performed in vacuum. The floor noise on top of the IP is reduced in the frequency range of the superattenuator resonances and the normal modes are almost completely damped.

Although the results are quite good on the IP, the actual performance of the inertial damping had to be measured on the mirror. A direct measurement of the residual motion of the mirror was possible by means of the 6 m test interferometer (CITF) now in operation on the VIRGO site (see [9]). Unfortunately, a measurement of the mirror motion with the inertial damping off is not possible, since the CITF cannot be locked in this situation. However, it is evident that inertial damping is necessary to lock the interferometer.

The CITF is a 6 m Michelson interferometer suspended from the final VIRGO superattenuators. The CITF is locked on a dark fringe by acting on one of the mirrors via its recoil mass. The CITF spectral sensitivity is the product of the spectrum of the correction force applied to the coils and the force-to-displacement transfer function between the coils and the controlled mirror. The result is a measurement of the free motion of the three masses.

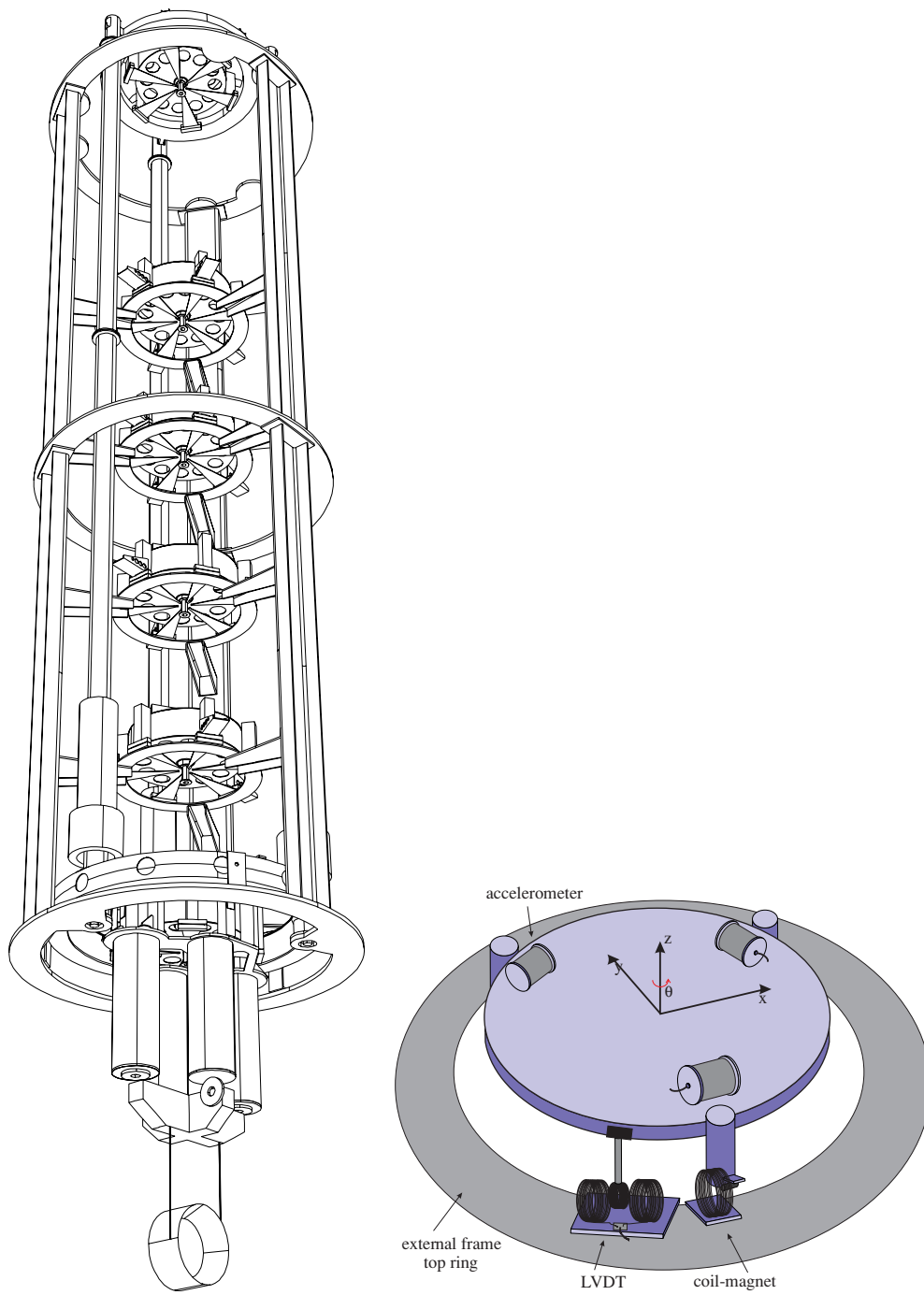


**Figure 1.** Left: VIRGO superattenuator. Right: simplified view of the IP top table, provided with the three accelerometers. One LVDT position sensor and one coil-magnet actuator are also shown. The  $X$ ,  $Y$ ,  $\Theta$  normal modes of the IP correspond approximately to translations along the  $\hat{x}$  and  $\hat{y}$  axes and rotation around the  $\hat{z}$  axis.

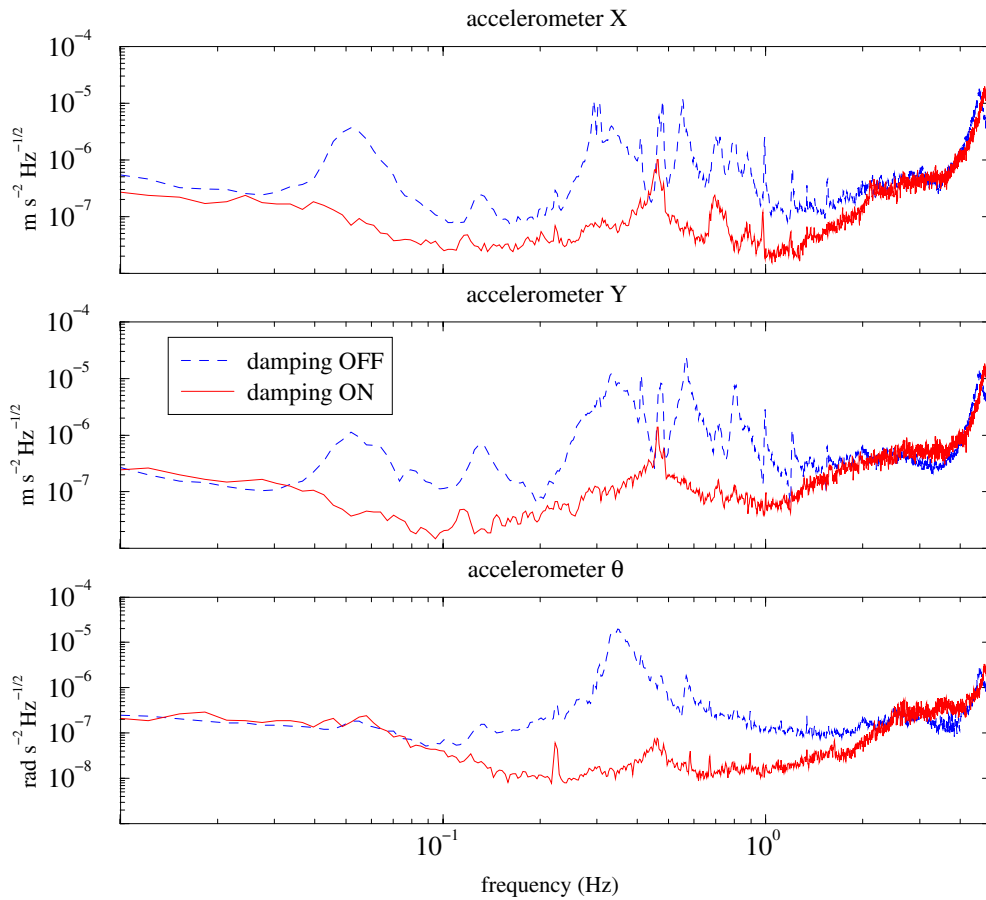


**Figure 2.** Performance of the inertial control ( $X, Y, \Theta$ ) of the superattenuator, measured on top of the IP as the output of the *virtual* accelerometer. The  $X, Y, \Theta$  normal modes correspond approximately to orthogonal translations on the plane and rotation around the vertical axis.

If we assume that the motions of the masses are uncorrelated, we can estimate the spectral motion of a single mirror as the CITF sensitivity divided by  $\sqrt{3}$ . The result is shown in figure 3.

The inertial damping reduces the amplitude of the SA resonant motions. Nevertheless, the spectrum of the mirror motions shows some resonance peaks. The presence of some of them can be explained by looking at the inverted pendulum force-to-displacement transfer function (see figure 3). This transfer function shows several dips, corresponding to frequencies where the gain of the inertial damping is less than unity (see [8]). The peak near 30 mHz has a different origin: 30 mHz is the frequency where the signals of the accelerometers and LVDT position sensors are blended to produce the error signal covering the entire control band. At this frequency the phase margin is reduced resulting in an excess of reinjected noise. This excess, as well as the low frequency drifts of the inverted pendulum, is compensated using the low frequency part of the CITF signal. This low frequency feedback is now active and will be the subject of a forthcoming paper [10].

The integrated rms motion is  $<0.1 \mu\text{m}$  in 10 s (figure 4). The rms velocity is  $<0.3 \mu\text{m s}^{-1}$ . This result has been obtained by integrating for 100 s, but a longer integration time does not change it.

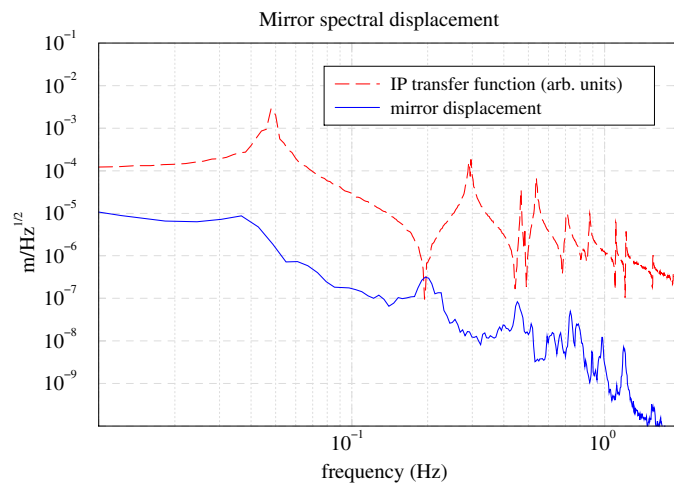


**Figure 3.** Linear spectrum of the mirror displacement  $\zeta(f)$  (solid line) measured by the VIRGO test interferometer compared with the force-to-displacement transfer function of the IP (dashed line). The transfer function has been measured by exciting the IP along the  $\hat{x}$  axis (using the *virtual* actuator  $\hat{x}$  and measuring the response with the corresponding  $\hat{x}$  displacement sensor). Some of the dips in the transfer functions correspond to peaks in the mirror spectrum.

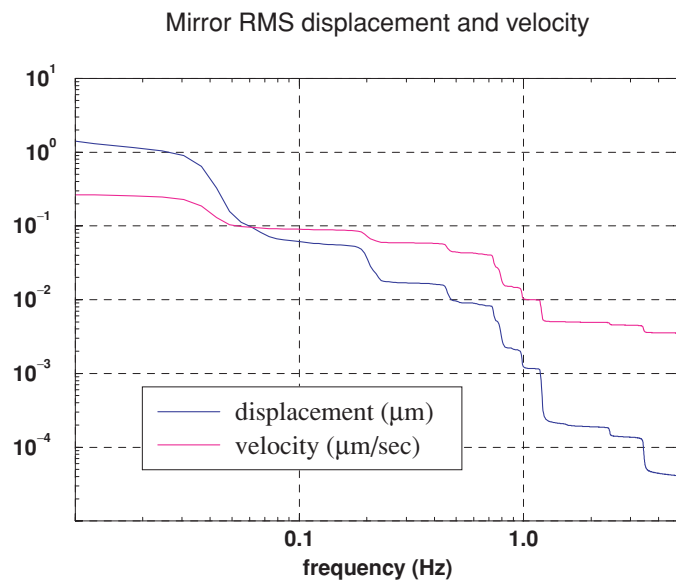


**Figure 4.** Integrated rms displacement calculated as  $\zeta_{\text{rms}}(f) = \left( \int_f^\infty \tilde{\zeta}(f)^2 df \right)^{1/2}$ . The corresponding rms mirror velocity is also plotted.

#### 4. The dynamic range of the marionette

The question arises, are these numbers small enough to keep the VIRGO interferometer in operation by acting on the marionette without re-injecting noise into the detection band? Since the residual motion of the mirror is known, one can try to define the bandwidth of the

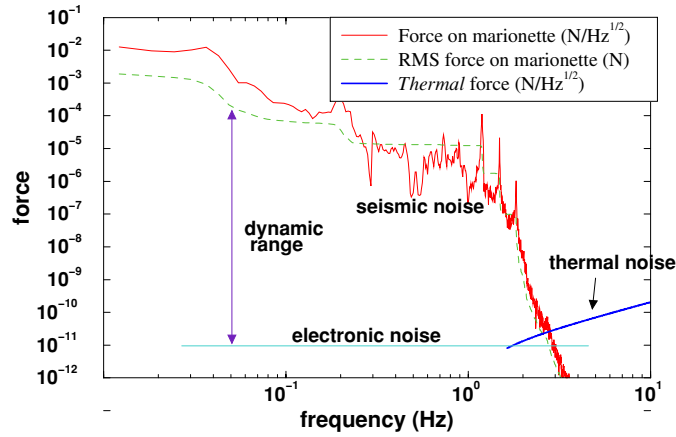


**Figure 5.** The plot shows the spectrum of the forces on the marionette needed to reproduce: the mirror seismic motion and the predicted thermal motion. The integrated rms force and the spectrum of the DAC electronic noise are also displayed. The dynamic range of the marionette control stage sets the lower frequency limit of the marionette action ( $\sim 50$  mHz).

control from the marionette. The best way to do it is thinking in terms of *force* rather than *displacement*. Let  $\tilde{\zeta}_m(f)$  be the measured spectral displacement of the mirror and  $G(f)$  the marionette–mirror force-to-displacement transfer function. Then

$$\tilde{F}(f) = \frac{\tilde{\zeta}_m(f)}{G(f)} \quad (1)$$

is the spectral force that would produce such a mirror displacement. Figure 5 shows  $\tilde{F}$  and the integrated rms force. The VIRGO target thermal noise [11] has also been plotted in terms of force from the marionette. The slope of the thermal force is positive because, around 10 Hz,  $\tilde{\zeta}_m(f) \propto f^{-5/2}$  (since the pendulum thermal noise dominates in this range), while  $G(f) \propto f^{-4}$  (since the mechanical system behaves as a double pendulum [5, 12]). Therefore  $G(f) \propto f^{3/2}$ .

The intersection between the two curves is the maximum spectral force that can be exerted from the marionette without injecting noise in the detection band. Therefore, the electronic noise associated with the control forces exerted from the steering filter–marionette actuators must be kept below that critical level. The system is designed to fulfil this requirement. Once the noise level is fixed, the dynamic range sets the maximum force. We define the dynamic range as

$$\tilde{D} = \frac{V_{\max}}{\tilde{V}_{\text{noise}}} = 2.5 \times 10^7 \sqrt{\text{Hz}} \quad (2)$$

where  $V_{\max} = 10$  V is the maximum voltage output of the DAC and  $\tilde{V}_{\text{noise}} = 0.4 \times 10^{-6} \text{ V Hz}^{-1/2}$  is the DAC noise level. The actuators must be designed in such a way to keep the corresponding force noise at the level of  $\sim 10^{-11} \text{ N Hz}^{-1/2}$ . The rms force that can be exerted from the marionette is then

$$F_{\text{rms}} \approx 2.5 \times 10^{-4} \text{ N} \quad (3)$$

corresponding to a maximum rms displacement of  $\sim 0.1 \mu\text{m}$ . Since the main contributions to the integrated rms force come from peaks in the spectrum, the maximum force can be calculated as

$$F_{\max} = \sqrt{2} \times F_{\text{rms}} \approx 3.5 \times 10^{-4} \text{ N}. \quad (4)$$

In terms of bandwidth, one can see from the plot that the marionette can be used to control the mirror down to about 50 mHz. Below 50 mHz the mirror position will be controlled from the inverted pendulum.

## 5. Conclusions

Inertial damping plays an important role in the control strategy reducing the maximum displacement to be compensated from the marionette and making it easier to design a simple two-stage control strategy. We have shown that the control of the VIRGO interferometer can be performed by acting on the marionette down to 50 mHz and on the inverted pendulum down to DC.

## References

- [1] Ballardin G *et al* 2001 Measurement of the VIRGO superattenuator performance for seismic noise suppression *Rev. Sci. Instrum.* **72** 3643
- [2] Fritschel P, Zucker M, Bork R, Mavalvala N, Ouimette D, Gonzalez G, Rong H and Sigg D 2000 Readout and control of a power recycled interferometric gravitational wave antenna *LIGO Internal Report LIGO-P-000008-A-D* web page <http://www.ligo.caltech.edu/docs/P/P000008-A.pdf>
- [3] Losurdo G *et al* 1999 An inverted pendulum pre-isolator stage for VIRGO suspension system *Rev. Sci. Instrum.* **70** 2507
- [4] Bernardini A, Majorana E, Puppo P, Rapagnani P, Ricci F and Testi G 1999 Suspension last stages for the mirrors of the VIRGO interferometric gravitational wave antenna *Rev. Sci. Instrum.* **70** 3463
- [5] Ballardin G *et al* 2001 Measurement of the transfer function of the steering filter of the VIRGO superattenuator suspension *Rev. Sci. Instrum.* **72** 3635
- [6] Braccini S *et al* 1995 Low noise wide band accelerometer using an inductive displacement sensor *Rev. Sci. Instrum.* **66** 2672
- [7] Tariq H *et al* 2001 The linear variable differential transformer (LVDT) position sensor for gravitational wave Interferometer low-frequency controls *Nucl. Instrum. Methods* submitted
- [8] Losurdo G *et al* 2001 Inertial control of the mirror suspensions of the VIRGO interferometer for gravitational wave detection *Rev. Sci. Instrum.* **72** 3653
- [9] Di Fiore L for the VIRGO Collaboration 2002 The status of the VIRGO central interferometer *Proc. of the 4th Edoardo Amaldi Conf. on Gravitational Waves (Perth, Western Australia, 8–13 July 2001)* *Class. Quantum Grav.* **19** 1421
- [10] Holloway L, Losurdo G and Passuello D 2001 Feedback of interferometer error signal to upper suspension *VIRGO Internal Report VIR-NOT-PIS-1390-182*
- [11] Punturo M 2001 The VIRGO sensitivity curve *VIRGO Internal Report VIR-NOT-PIS-1390-51* webpage <http://www.virgo.infn.it/senscurve/VIR-NOT-PER-1390-51.pdf>
- [12] Bozzi A *et al* 2001 Last stage control and mechanical transfer function measurement of the VIRGO suspensions *Rev. Sci. Instrum.* submitted